IEEE Access
Multidisciplinary | Rapid Review | Open Access Journal

Received July 6, 2020, accepted August 2, 2020, date of publication August 7, 2020, date of current version August 19, 2020.

Digital Object Identifier 10.1109/ACCESS.2020.3014941

Sustaining the Radiation Properties of a 900-MHz-Band Planar LoRa Antenna Using a 2-by-2 Thin EBG Ground Plane

GEONYEONG SHIN[1], (Graduate Student Member, IEEE), TAE RIM PARK[2], JOOMIN PARK[1], (Student Member, IEEE), SANG-KYU LEE[3], GYUYONG KIM[3], AND ICK-JAE YOON[1], (Member, IEEE)

[1]Department of Electrical Engineering, Chungnam National University, Daejeon 34134, South Korea
[2]Ino-on Inc., Seoul 06247, South Korea
[3]Department of Architectural Engineering, Chungnam National University, Daejeon 34134, South Korea

Corresponding author: Ick-Jae Yoon (ijyoon@cnu.ac.kr)

This work was supported by Chungnam National University (CNU), Daejeon, South Korea, under Grant 2019-0687-01.

ABSTRACT In this work, a 2-by-2 array of a low-profile EBG ground plane is used as a means of sustaining the radiation performance of a 900-MHz LoRa antenna that could be installed at various construction sites. The proposed semi-circles added mushroom (SAM) structure enables a thin EBG height of 0.02λg on an FR-4 substrate at 900 MHz frequencies. A planar electric meander antenna for the 900-MHz LoRa band is integrated with the proposed 2-by-2 SAM plane. From a simulation and demonstration, it is found that the impedance and radiation properties of the integrated prototype in free space are well maintained with a minimum degradation even when it is placed on a concrete medium.

INDEX TERMS Internet of Things, LoRa, low-profile, planar antenna, electromagnetic band gap.

I. INTRODUCTION

There has been a great effort to realize the concept of an ''Internet of Things'' (IoT), which is composed of the series of processes of identifying, sensing, networking, and computation [1]–[3]. However, the active use of an IoT service is still limited by several concerns including security, battery life, and communication range. Modern low-power, wide-area networks (LPWAN) have been actively discussed over the last few years as a means of resolving such problems and LoRa (for ''long range'') is one of the representative technologies in the LPWAN domain that follows non-cellular protocols. It can cover a wide area of communication range with relatively low-power consumption and would enable the construction of highly connected future communication services [4]. One creative usage of this dense communication network is found in the field of construction work where the operation of equipment at unapproved times can be checked continuously to prevent potential accidents.

Fig. 1 shows a commercial LoRa device from Ino-on Inc. [5] that can detect the operation of a machine and the start of construction by recognizing and analyzing specific information through a network of sensors. It can be installed on a wall, pipe, or even in the field at construction sites and transmits a recognition signal to the access point once the operation of the equipment is detected by the incorporated vibration sensor. As shown in the figure, LoRa devices can be installed in a variety of environments, including on metal, ground surfaces, and concrete. The problem is that these environmental factors inevitably affect the antenna performance such as with the radiation pattern, radiation efficiency, and

FIGURE 1. Installation of a LoRa device with a vibration detection sensor in various environments. The device is highlighted with a yellow color for easy identification in the photos.

The associate editor coordinating the review of this manuscript and approving it for publication was Haiwen Liu.

impedance matching for the wireless communication [6], [7]. In general, low-cost, high-efficiency, small-size, and low-profile characteristics are required for LoRa antennas. Furthermore, an electrical robustness to the dynamic electromagnetic environments of the installation surroundings is strongly desired so that the antennas can be easily applied to various installation surface conditions with a minimal degradation of the radiation performance and can play a role in maximizing the total system efficiency.

The radiation efficiency and pattern of an electric dipole antenna standing parallel to a metal ground could be distorted since the electric current over the antenna is canceled by the 180° out-of-phase reflection of the common metal surface [8]. To move the antenna away from the ground or to locate the antenna vertically to the ground is not a proper solution since it prevents a low-profile design. Instead, a metal plane exhibiting an in-phase reflection could be used. Thus, an electromagnetic band gap (EBG) structure with a reflection phase within the range of $-180°$ to $180°$ has been applied to low-profile antenna designs [9]–[13]. Its use in the 900-MHz band is rather restricted, however, due to its thickness when designed for an inexpensive substrate such as an FR-4.

In this paper, we design a reduced-height metal plane showing the EBG characteristic at the 900-MHz-LoRa band on an FR-4 substrate. It is found that the resonant characteristic and the desired radiation pattern of a stand-alone planar meandered monopole LoRa antenna are still maintained even when it is put either on a corridor or a concrete block, after it is backed by a 2-by-2 array of the proposed metal plane. This paper is composed as follows. First, we show that the EBG characteristic can be achieved at a thinner substrate height by a modification of a common mushroom EBG structure. The phase range of $-180°$ to $180°$ is used for fair comparison with other works in the literature. Next, its 2-by-2 array is applied at the bottom of a LoRa communication PCB containing the planar meander monopole. In this procedure, the proposed metal plane is tuned a little to show the quadratic-phase reflection (range $90° \pm 45°$) for its best use in antennas in terms of impedance matching and radiation pattern [9]. The computed expectations in this work are verified experimentally.

II. ANTENNA WITH LOW-PROFILE EBG STRUCTURE

As a means of maintaining the radiation properties of a LoRa antenna at an installation site, we propose to add an electrically and physically thin, small metal plane exhibiting a specific reflection phase property between the LoRa PCB and the external installation environment as described in Fig. 2a. The additional metal plane should have a low profile to maintain within reason the short height of the entire LoRa device, and its other dimensions should be about the same as the device platform. A low fabrication cost is also required to be used for a massive number of LoRa devices. Figs. 2b and 2c show a more detailed description of the LoRa device used in this work. The diameter of the housing disk is 10 cm with a thickness of 1 cm, in which the batteries and

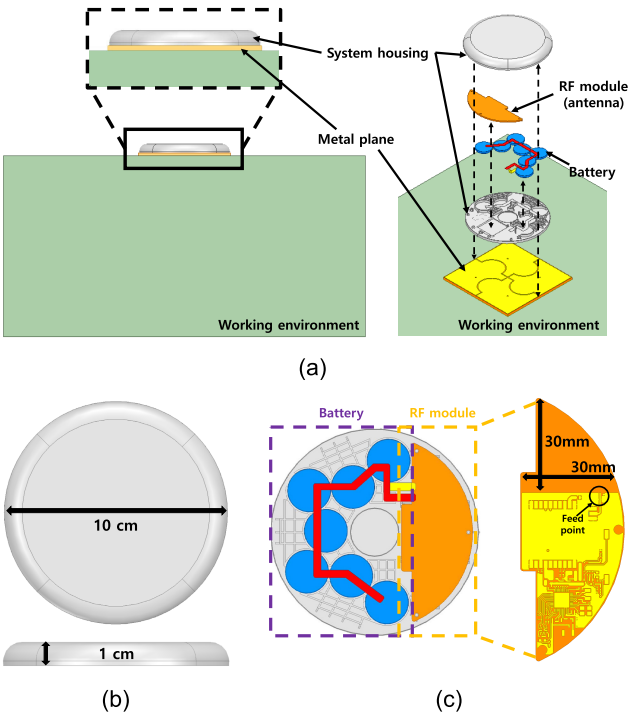

FIGURE 2. Description of the LoRa device. (a) Working environment and the internal configuration of the LoRa device. (b) Top and side views of the device housing. (c) Inside of the device consisting of a battery and RF module.

radio frequency (RF) module are located. The RF module is allocated at the side; thus, a space of less than 30×30 mm^2 is allowed for a LoRa antenna. In Section II-A, an electrically and physically thin EBG is designed by the modification of the mushroom EBG structure on an FR-4 substrate. For the antenna design in the limited space, we use a stub-loaded meander antenna [14]–[18]. Its design with the proposed 2-by-2 array of the metal plane is discussed in Section II-B. The radiation performance of the proposed antenna backed by the metal plane is shown in Section II-C.

A. DESIGN OF LOW-PROFILE EBG STRUCTURE

The EBG structure consists of a periodic array of a specific sub-wavelength metal structure, often referred to as a unit cell, and is generally classified as a metamaterial [9]. The quadratic- or in-phase reflection of the EBG structure along the frequency can be used as a ground conductor for an electric dipole standing parallel to it [19], [20]. EBGs operating below a frequency range of 1 GHz usually have relatively complex structures or have been designed on expensive substrates whose dielectric constant is more than 10 for miniaturization [21]–[24]. As an alternative, we propose to reduce the height of the mushroom EBG structure [9] whose resonant frequency is determined by the inductance (L) from the shorting pin and the coupling capacitance (C) between the adjacent cells as shown in Fig. 3a. The resonance frequency

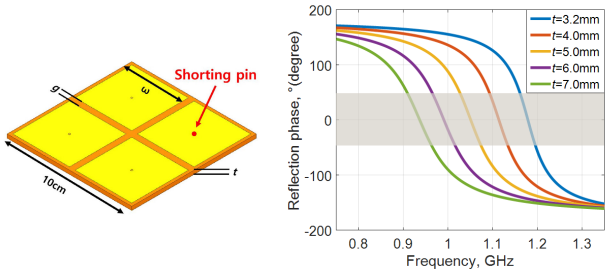

FIGURE 3. Conventional mushroom EBG. (a) Mushroom EBG structure on an FR-4 ($\varepsilon_r = 4.4$, $tan\delta = 0.02$) substrate. Its 2-by-2 array is shown. (b) Reflection phase response according to the thickness of the substrate (t) when a periodic boundary condition is applied in the simulation.

(ω_0) is determined as [20] follows:

$$\omega_0 = \frac{1}{\sqrt{LC}} \tag{1}$$

As clearly shown from (1), the resonant frequency is lowered when L and C become higher. Usually, the L of the unit cell can be increased with an electrically longer shorting pin, and C can be increased with a larger patch width (w), a higher dielectric constant of the substrate, and a smaller gap between the cells (g) [9]. In other words, a thicker substrate thickness (t) or a longer length of the adjacent edges between the cells shifts the operating frequency down or reduces the size of the EBG design. With a w of 4.9 cm and a g of 0.1 cm on an FR-4 substrate, we first carry out a parameter study on the reflection phase with the substrate thickness t as shown in Fig. 3b using the cells in Fig. 3a with a periodic boundary condition. It is clearly seen that the operating frequency decreases as t increases. It is also observed that the mushroom structure needs at least a 7 mm thickness to operate near 900 MHz. However, 7 mm is not a standard value from the commercially available substrates and is also quite thick. Therefore, we insert a semi-circular shape as shown in Figs. 4a and 4b. It increases the facing area between the adjacent cells and could make the C higher without changing the physical dimensions of 10 × 10 cm^2 for the 2-by-2 array of the conventional mushroom structure in Fig. 3a. The change of the reflection phase according to D is plotted in Fig. 4c, when t is fixed at 3.2 mm. As observed, it could satisfy the 900 MHz LoRa operating frequency band in the same dimension without increasing the dielectric constant. Compared to the result in Fig. 3b, the thickness could be reduced by about 55% (i.e., t is decreased from 7.0 mm to 3.2 mm) when the diameter of the semicircular structure D is 48 mm. The conventional mushroom could meet an operating frequency of 1.18 GHz when $t = 3.2$ mm.

Thus, the same miniaturization effect of the increased thickness is achieved by introducing the semi-circular shape into the mushroom structure. Table 1 compares the EBGs designed for the frequency below 1 GHz in the literature with this work in terms of thickness, dielectric constant, bandwidth, and resonant frequency, when the cells are in an infinitely large array. It is clearly seen that the proposed EBG structure shows the thinnest profile, except for [22] which used a substrate with a relative permittivity of 100. In addition, the resonance frequency of the proposed structure can be easily adjusted by tuning D. Such a feature could be effectively used in matching the operating frequency when it is integrated with antennas, as is discussed in Section II-B.

TABLE 1. Comparison of EBG structures designed for an operating frequency below 1 GHz.

Ref.	Thickness [mm]	Relative permittivity	Bandwidth [%]	Resonance frequency
[21]	5.08 (0.09λ_g)	36	6.29	0.888 GHz
[22]	0.58 (0.005λ_g)	100	< 1	0.247 GHz
[23]	13 (0.11λ_g)	13	7.1	0.712 GHz
[24]	2.54 (0.036λ_g)	25	4.38	0.868 GHz
This Work	3.2 (0.02λ_g)	4.4	2.2	0.901 GHz

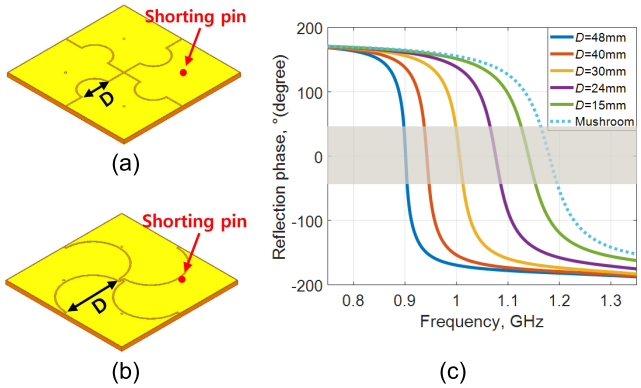

FIGURE 4. Proposed, semi-circles added mushroom (SAM) EBG. (a) SAM EBG on an FR-4 ($t = 3.2$ mm) substrate, $D = 24$ mm, (b) SAM EBG on an FR-4 ($t = 3.2$ mm) substrate, $D = 48$ mm. (c) Reflection phase response according to D when a periodic boundary condition is applied in the simulation.

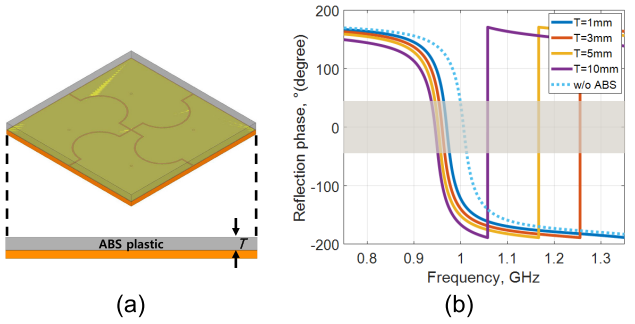

FIGURE 5. Effect of the housing material. (a) Proposed semi-circles added to the mushroom EBG structure with a specific thickness (T) of ABS plastic ($\varepsilon_r = 2.0$ and $tan\delta = 0.019$) $D = 30$ mm. (b) Reflection phase response according to T when a periodic boundary condition is applied in the simulation.

B. ANTENNA BACKED BY A 2-BY-2 EBG STRUCTURE

In this sub-section, a planar meander antenna for a 900 MHz LoRa band and the 2-by-2 array of the semi-circle added

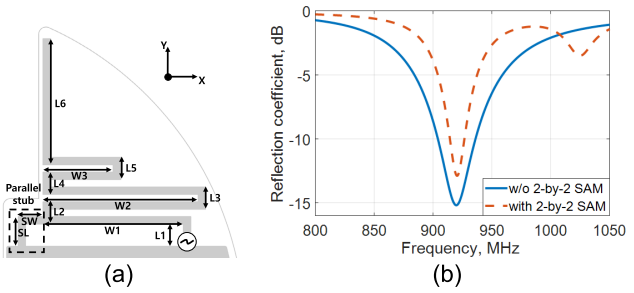

FIGURE 6. Planar, meandered LoRa antenna. (a) Antenna description. (b) Simulated reflection coefficients of the designed antenna considering the system housing and the antenna with 2-by-2 semi-circles added to the mushroom at the bottom. The latter one is obtained after a slight tuning.

mushroom (SAM) are tuned for integration. As was shown in Fig. 2, the 2-by-2 SAM is located between the LoRa PCB containing the antenna and the installation surface. The proposed SAM itself has relatively smaller electromagnetic effects from the installation medium due to its grounding conductor at the bottom. As a first step of integration, we place an ABS plastic ($\varepsilon_r = 2.0$, $tan\delta = 0.019$) with a specific thickness of T on top of the SAM as shown in Fig. 5a and observe the reflection phase. ABS plastic is used for the fabrication of the system housing. As shown in Fig. 5b, the operating frequency is lowered in the presence of the ABS plastic.

The EBG structure operates like a perfect magnetic conductor (PMC) near the resonance frequency showing the reflection phase of 0° with the continuous reflection phase variation from −180° to 180° across the frequency. However, it is not easy to achieve sufficient impedance matching with an antenna placed on top of the PMC due to the strong mutual coupling between the antenna and the PMC. Instead, as was thoroughly discussed in [9], an EBG structure exhibiting a quadratic-phase reflection acts better in impedance matching and efficient radiation. For this reason, we tune the SAM in the presence of the housing material to meet the quadratic-phase response. In Fig. 5b, the reflection phase is nearly 45° at the target center frequency of 920 MHz when T is 10 mm, which is the thickness of the system housing (see Fig. 2b). D is fixed at 30mm.

The space allowed for the antenna is only about half of 30 × 30 mm^2. Under this design condition, a planar, meandered monopole antenna is chosen as shown in Fig. 6a to ensure the electrical length of resonance in the target frequency. A parallel stub is loaded to step up its low radiation resistance from the relatively short length from the ground along the y-axis to a 50 ohm. No additional lumped elements are used for matching circuitry to avoid any possible additional loss to the antenna resistance. Although an antenna design method using a parallel stub is not proper for its Q-factor that is approaching the theoretical lower physical bound of electrically small antennas [25], such an inverted-F design technique has been successfully implemented in antenna designs when the space given to antenna allocation is tightly limited [26]–[28].

TABLE 2. Final antenna design parameters.

Parameter	Value	Parameter	Value	Parameter	Value
L1	3	L5	3	W1	19
L2	3	L6	17	W2	21
L3	3	SW	3.38	W3	9.5
L4	3	SL	4		

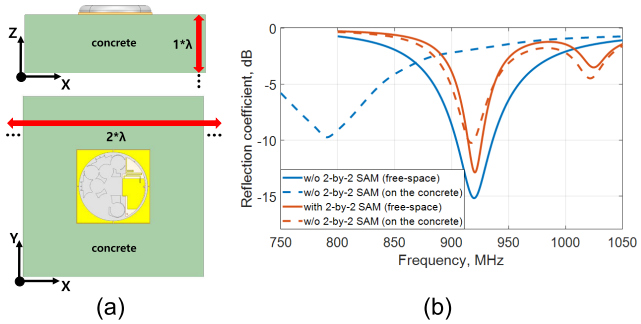

FIGURE 7. Designed LoRa antenna with environment. (a) Side and top views of the proposed 2-by-2 SAM applied to the LoRa device when it is on a homogeneous material box of concrete ($\varepsilon_r = 6.57$, $tan\delta = 0.0536$). (b) Reflection coefficients.

The antenna covering part of the 900-MHz Lora frequencies from the United States (902-928 MHz) and Korea (921.9–923.3 MHz) [29] is designed on an FR-4 substrate with the thickness of 1.6 mm. Considering the material properties of the system housing, meander line, and parallel stub are tuned to be matched in the LoRa frequency band as can be shown by the solid blue line in Fig. 6b. After checking its self-resonant characteristic, the antenna design parameters are further tuned to resonate at the target center frequency in the presence of the 2-by-2 SAM with quadratic-phase reflection. Fig. 6a shows a final description of the antenna with the 2-by-2 SAM beneath it. The values of the design parameters are summarized in Table 2. The width of all the lines is 1 mm.

C. ANTENNA PERFORMANCE ON THE CONCRETE MATERIAL

Now, the impedance matching and radiation performance of the meander antenna backed with the proposed 2-by-2 SAM are analyzed when it is on a homogeneous medium mimicking the concrete ($\varepsilon_r = 6.57$, $tan\delta = 0.0536$ [30]), one possible location at a construction site. The dimensions of the homogeneous concrete medium in Fig. 7a is 65 × 65 cm^2 with a thickness of 32.5 cm.

The simulated reflection coefficients of the LoRa antenna with and without the 2-by-2 SAM are plotted in Fig. 7b, for the cases in which it stands alone in free-space and when located on top of the concrete medium. As shown in Fig. 7b, the resonant frequency shifts down to 791 MHz due to the dielectric properties of the concrete when the antenna is not backed by the 2-by-2 SAM, whereas it stays almost the same but decreases very slightly to 917.5 MHz from 920 MHz when the antenna is backed by the 2-by-2 SAM. Moreover, as shown in Fig. 8a, the LoRa antenna with the proposed

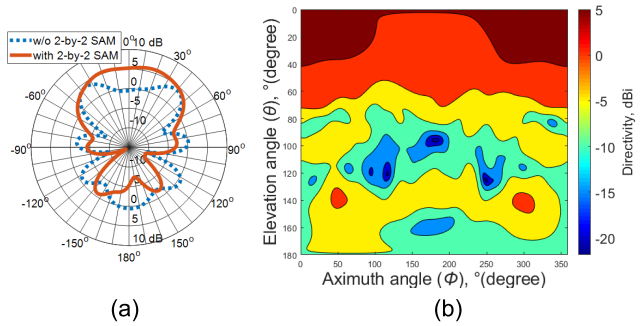

FIGURE 8. Simulated total radiation patterns of the LoRa antenna on the concrete box material. (a) Radiation pattern in the *yz*-plane. (b) 2D pattern of the antenna with the 2-by-2 SAM in-between the antenna and the concrete material.

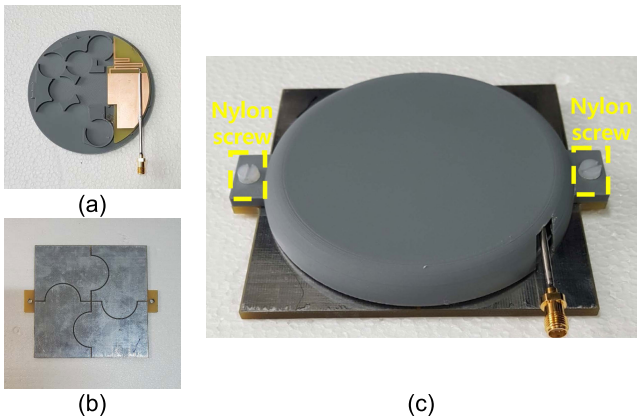

FIGURE 9. Built prototype. (a) Built LoRa antenna on an FR-4 substrate (1.6 mm). (b) Proposed 2-by-2 SAM on an FR-4 substrate (3.2 mm). (c) Assembly of the antenna and the 2-by-2 SAM with 3D-printed housing.

2-by-2 SAM shows a directional beam pattern toward the broadside (i.e., toward the positive z-axis), which is more suitable for the reliable wireless communication service of the LoRa. From the blue dashed line, it is also clearly seen that the total radiation pattern of the LoRa antenna without the 2-by-2 SAM is more dispersive to the concrete medium. Lastly, it is observed that the directional beam pattern of the antenna with the 2-by-2 SAM is formed over the entire azimuth plane, as shown in Fig. 8b.

III. FABRICATION AND MEASUREMENT

A prototype of the LoRa antenna backed by the 2-by-2 SAM is built, and its performance of maintaining the radiation properties is demonstrated. Fig. 9 shows the photos of the built prototype. The plastic housing is printed from ABS filament using a fused deposition modeling (FDM) 3D printer from Zortrax (Model M200). The metals of the antenna and the 2-by-2 SAM are patterned on each FR-4 substrate with a thickness of 1.6 mm and 3.2 mm, respectively. As shown in Fig. 9c, nylon screws are used to assemble the 2-by-2 SAM and the housing.

For the demonstration, first, the built prototype is placed on a common corridor of concrete ground as shown in Fig. 10a,

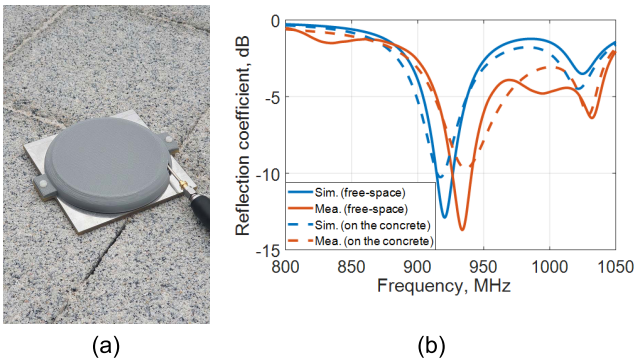

FIGURE 10. Performance validation of the built prototype on a corridor. (a) Measurement photo. (b) Reflection coefficients.

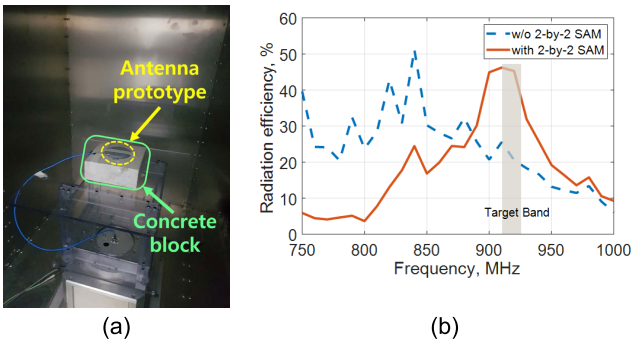

FIGURE 11. Radiation efficiency measurement. (a) Built prototype in a reverberation chamber with a concrete block of 20 × 20 × 8 cm^3 (b) Measured radiation efficiencies.

and its reflection coefficient is measured using a vector network analyzer (Anritsu MS46522B). The blue and red solid lines in Fig. 10b show the simulated free-space and measured reflection coefficient, respectively. The measured center frequency is shifted slightly upward to 933.5 MHz compared to the simulation result of 920.5 MHz. This is possibly caused by a lower dielectric constant of the FDM-based 3D-printed housing, where the filaments are stacked sequentially to create a three-dimensional structure. When the layers are not fully populated thus allowing air in between, the expected dielectric constant could be less [31], [32]. Nevertheless, the LoRa frequency band is still covered with a −6 dB criterion and more importantly, as shown by the dashed lines in Fig. 10b, the resonant frequency is only shifted by 3 MHz even when the antenna is on the concrete surface, for both the simulation and measurement. It is thus confirmed that the impedance characteristic of the antenna could be well secured by the antenna backed by the proposed, thin 2-by-2 SAM structure.

Next, the radiation efficiency of the built prototype is tested while it is placed on a concrete block of 20 × 20 × 8 cm^3. We carry out the measurement in an electromagnetic reverberation chamber (RC) as shown in Fig. 11a. An RC is a shielded enclosure that is generally equipped with mechanical stirrers that change the boundary condition, providing a signal source of randomly polarized, spatially

TABLE 3. Characteristics of the LoRa antenna according to the presence or absence of proposed metal plane.

	Without proposed 2-by-2 SAM	With proposed 2-by-2 SAM
Impedance matching (free space)	O	O
Impedance matching (concrete)	X	O
Directivity	4.4 dBi (non-directional)	5.8 dBi (directional)
Radiation efficiency (@ 920 MHz)	20.5%	45.2 %

uniform, and isotropic inside the RC, making it easier to measure the radiation efficiency of the antenna under test (AUT) [33]. In addition, unlike the measurement setup in an anechoic chamber, the AUT can be simply put on a rig and physically fixed. It is more suitable to measure the AUT sample with the heavy concrete block like this work, which is 6.3 kg. Fig. 11b shows the measured radiation efficiency of the antenna prototype with and without the presence of the proposed 2-by-2 SAM. It is found that the built prototype without the 2-by-2 SAM shows a maximum radiation efficiency around 840 MHz, which is much lower than the original operating frequency of 920 MHz. The prototype with the 2-by-2 SAM still shows a radiation efficiency of 45.2% at the target frequency of 920 MHz. It is worth noting that this is more than twice that of the antenna without the 2-by-2 SAM, which is only 20.5% at the same frequency. We thus verify the usefulness of the proposed prototype as a means of maintaining the radiation properties of the antenna without much increase in the thickness of the device. The key results are compared in Table 3.

IV. CONCLUSION

In this paper, a method for reducing the height of the mushroom EBG structure was proposed and a 2-by-2 piece of the array, named SAM, was used under a planar meander monopole antenna as a means of minimizing the surrounding electromagnetic effects when the antenna is installed at construction sites. All these works were carried out for the 900-MHz LoRa frequencies. Being different from the previous works using high permittivity materials for EBG structure miniaturization, it was shown that the proposed method is relatively simpler and easy to use with a cheap fabrication cost. It is thus suitable for applications where many sensors are to be distributed, like LoRa.

It is worth noting that the 2-by-2 SAM does not show a perfect EBG characteristic as it is not periodically arrayed enough but is rather properly a metamaterial-inspired metal plane. Nevertheless, it was shown that the meander LoRa antenna backed by the 2-by-2 SAM could maintain its radiation properties when it was placed on possible construction site environments. Such performance was tested in simulation with a homogeneous concrete block and demonstrated in a corridor and on a real concrete block. The results from the simulation, demonstration, and the RC measurement showed that the radiated beam was not dispersive to the installation ground but directive toward the broadside direction, and the resonance characteristic was maintained with a good radiation efficiency.

REFERENCES

[1] A. Čolaković and M. Hadžialić, "Internet of Things (IoT): A review of enabling technologies, challenges, and open research issues," *Comput. Netw.*, vol. 144, pp. 17–39, Oct. 2018.

[2] J. M. Talavera, L. E. Tobón, J. A. Gómez, M. A. Culman, J. M. Aranda, D. T. Parra, L. A. Quiroz, A. Hoyos, and L. E. Garreta, "Review of IoT applications in agro-industrial and environmental fields," *Comput. Electron. Agricult.*, vol. 142, pp. 283–297, Nov. 2017.

[3] S. M. R. Islam, D. Kwak, M. H. Kabir, M. Hossain, and K.-S. Kwak, "The Internet of Things for health care: A comprehensive survey," *IEEE Access*, vol. 3, pp. 678–708, 2015.

[4] LoRa Alliance, Fremont, CA, USA. (Nov. 1, 2015). *What is LoRaWAN*. Accessed: May 16, 2020. [Online]. Available: https://lora-alliance.org/resource-hub/what-lorawanr

[5] Ino-On. *About Ino-Vive*. Accessed: May 16, 2020. [Online]. Available: https://www.ino-on.co.kr/about-ino-vibe

[6] S.-H. Jeong and H.-W. Son, "UHF RFID tag antenna for embedded use in a concrete floor," *IEEE Antennas Wireless Propag. Lett.*, vol. 10, pp. 1158–1161, Oct. 2011.

[7] J. D. Griffin, G. D. Durgin, A. Haldi, and B. Kippelen, "RF tag antenna performance on various materials using radio link budgets," *IEEE Antennas Wireless Propag. Lett.*, vol. 5, pp. 247–250, Dec. 2006.

[8] C. A. Balanis, *Antenna Theory: Analysis and Design*, 3rd ed. New York, NY, USA: Wiley, 2005, pp. 197–204.

[9] F. Yang and Y. Rahmat-Samii, "Reflection phase characterizations of the EBG ground plane for low profile wire antenna applications," *IEEE Trans. Antennas Propag.*, vol. 51, no. 10, pp. 2691–2703, Oct. 2003.

[10] J. B. Bell and M. F. Iskander, "A low-profile archimedean spiral antenna using an EBG ground plane," *IEEE Antennas Wireless Propag. Lett.*, vol. 3, pp. 223–226, Oct. 2004.

[11] S. Xuat Ta and I. Park, "Dual-band low-profile crossed asymmetric dipole antenna on dual-band AMC surface," *IEEE Antennas Wireless Propag. Lett.*, vol. 13, pp. 587–590, Mar. 2014.

[12] H. Malekpoor and S. Jam, "Improved radiation performance of low profile printed slot antenna using wideband planar AMC surface," *IEEE Trans. Antennas Propag.*, vol. 64, no. 11, pp. 4626–4638, Nov. 2016.

[13] S. Nelaturi and N. V. S. N. Sarma, "A compact microstrip patch antenna based on metamaterials for Wi-Fi and WiMAX applications," *J. Electromagn. Eng. Sci.*, vol. 18, no. 3, pp. 182–187, Jul. 2018.

[14] J.-S. Sun, H.-S. Fang, P.-Y. Lin, and C.-S. Chuang, "Triple-band MIMO antenna for mobile wireless applications," *IEEE Antennas Wireless Propag. Lett.*, vol. 15, pp. 500–503, Jul. 2015.

[15] S.-L. Zuo, Z.-Y. Zhang, and J.-W. Yang, "Planar meander monopole antenna with parasitic strips and sleeve feed for DVB-H/LTE/GSM850/900 operation in the mobile phone," *IEEE Antennas Wireless Propag. Lett.*, vol. 12, pp. 27–30, Dec. 2013.

[16] A. Kiourti and K. S. Nikita, "Miniature scalp-implantable antennas for telemetry in the MICS and ISM bands: Design, safety considerations and link budget analysis," *IEEE Trans. Antennas Propag.*, vol. 60, no. 8, pp. 3568–3575, Aug. 2012.

[17] D.-O. Ko and J.-M. Woo, "Design of a small radio frequency identification tag antenna using a corrugated meander line applicable to a drug runout sensor system," *J. Electromagn. Eng. Sci.*, vol. 18, no. 1, pp. 7–12, Jan. 2018.

[18] S. Kim and H. Shin, "An ultra-wideband conformal meandered loop antenna for wireless capsule endoscopy," *J. Electromagn. Eng. Sci.*, vol. 19, no. 2, pp. 101–106, Apr. 2019.

[19] F.-R. Yang, K.-P. Ma, Y. Qian, and T. Itoh, "A uniplanar compact photonic-bandgap (UC-EBG) structure and its applications for microwave circuits," *IEEE Trans. Microw. Theory Tech.*, vol. 47, no. 8, pp. 1509–1514, Aug. 1999.

[20] D. Sievenpiper, L. Zhang, R. F. J. Broas, N. G. Alexópolous, and E. Yablonovitch, "High-impedance electromagnetic surfaces with a forbidden frequency band," *IEEE Trans. Microw. Theory Techn.*, vol. 47, no. 11, pp. 2059–2074, Nov. 1999.

[21] D. J. Kern, D. H. Werner, A. Monorchio, L. Lanuzza, and M. J. Wilhelm, "The design synthesis of multiband artificial magnetic conductors using high impedance frequency selective surfaces," *IEEE Trans. Antennas Propag.*, vol. 53, no. 1, pp. 8–17, Jan. 2005.
[22] D. J. Kern, M. J. Wilhelm, D. H. Werner, and P. L. Werner, "A novel design technique for ultra-thin tunable EBG AMC surfaces," in *Proc. IEEE AP-S/URSI Symp.*, Monterey, CA, USA, Jun. 2004, pp. 1167–1170.
[23] M. Hosseini, A. Pirhadi, and M. Hakkak, "Design of a novel AMC with little sensitivity to the angle of incidence and very compact size," in *Proc. IEEE AP-S/URSI Symp.*, Albuquerque, NM, USA, Jul. 2006, pp. 1939–1942.
[24] M. E. de Cos, F. Las Heras, and M. Franco, "Design of planar artificial magnetic conductor ground plane using frequency-selective surfaces for frequencies below 1 GHz," *IEEE Antennas Wireless Propag. Lett.*, vol. 8, pp. 951–954, Aug. 2009.
[25] S. R. Best, "Low Q electrically small linear and elliptical polarized spherical dipole antennas," *IEEE Trans. Antennas Propag.*, vol. 53, no. 3, pp. 1047–1053, Mar. 2005.
[26] H. F. AbuTarboush, R. Nilavalan, T. Peter, and S. W. Cheung, "Multi-band inverted-F antenna with independent bands for small and slim cellular mobile handsets," *IEEE Trans. Antennas Propag.*, vol. 59, no. 7, pp. 2636–2645, Jul. 2011.
[27] Y. Li, Z. Zhang, J. Zheng, Z. Feng, and M. F. Iskander, "A compact hepta-band loop-inverted f reconfigurable antenna for mobile phone," *IEEE Trans. Antennas Propag.*, vol. 60, no. 1, pp. 389–392, Jan. 2012.
[28] K.-L. Wong and C.-Y. Tsai, "Small-size stacked inverted-F antenna with two hybrid shorting strips for the LTE/WWAN tablet device," *IEEE Trans. Antennas Propag.*, vol. 62, no. 8, pp. 3962–3969, May 2014.
[29] S. Lee, H. Yoon, K.-J. Baik, and B.-J. Jang, "Emulator for generating heterogeneous interference signals in the Korean RFID/USN frequency band," *J. Electromagn. Eng. Sci.*, vol. 18, no. 4, pp. 254–260, Oct. 2018.
[30] W. B. Westphal and A. Sils, "Dielectric constant and loss data," United States Air Force Mater. Lab., Wright-Patterson AFB, OH, USA, Tech. Rep. AFML-TR-72-39, Apr. 1972.
[31] S. Zhang, Y. Vardaxoglou, W. Whittow, and R. Mittra, "3D-printed flat lens for microwave applications," in *Proc. Loughborough Antennas Propag. Conf. (LAPC)*, Nov. 2015, pp. 1–3.
[32] S. Moscato, R. Bahr, T. Le, M. Pasian, M. Bozzi, L. Perregrini, and M. M. Tentzeris, "Infill-dependent 3-D-printed material based on NinjaFlex filament for antenna applications," *IEEE Antennas Wireless Propag. Lett.*, vol. 15, pp. 1506–1509, Jan. 2016.
[33] P.-S. Kildal and K. Rosengren, "Correlation and capacity of MIMO systems and mutual coupling, radiation efficiency, and diversity gain of their antennas: Simulations and measurements in a reverberation chamber," *IEEE Commun. Mag.*, vol. 42, no. 12, pp. 104–112, Dec. 2004.

GEONYEONG SHIN (Graduate Student Member, IEEE) received the B.S. and M.S. degrees in electrical engineering from Chungnam National University, Daejeon, South Korea, in 2017 and 2019, respectively, where he is currently pursuing the Ph.D. degree in electrical engineering. His research interests include antennas and theoretical methods for electromagnetics.

TAE RIM PARK received the Ph.D. degree in electronic engineering and computer science from Seoul National University, Seoul, South Korea. He is currently a Co-Founder and the CEO of Inoon Inc. Before starting the startup company, he has worked as a Senior Research Engineer for the Samsung Advanced Institute of Technology, Samsung Electronics Company Ltd., Yongin, South Korea, from 2008 to 2014. From 2005 to 2008, he has worked for the City University of New York as a Researcher. His current research interests include low power wide area networks, ultralow power system design, and tiny machine learning for resource constrained small devices.

JOOMIN PARK (Student Member, IEEE) received the B.S. degree in radio science engineering from Kongju National University, Cheonan, South Korea, in 2016. He is currently pursuing the M.S. degree in electrical engineering with Chungnam National University, Daejeon, South Korea. His research interests include antennas and high frequency modeling of motors for EMC test.

SANG-KYU LEE received the B.S. and M.S. degrees in architectural engineering from Chungnam National University, Daejeon, South Korea, in 2015 and 2017, respectively, where he is currently pursuing the Ph.D. degree in architectural engineering. His research interests include impact resistance and EMP shielding performance of fiber reinforced cementitious composites.

GYUYONG KIM received the Ph.D. degree in architectural engineering from Chungnam National University (CNU), Daejeon, South Korea, in 1999. From 1999 to 2002, he worked as a Researcher with the Building Research Institute of Japan (BRI). From 2002 to 2005, he worked for the building material group of Samsung C&T Corporation Institute of Technology. Since 2005, he has been a Professor with the Department of Architectural Engineering, CNU. From 2014 to 2015, he has visited the State University of New Jersey, Rutgers, as a Visiting Scholar. His current research interests include impact resistance, explosion resistance, EMP protection of cementitious composites, fire-resistance concrete, self-shrinkage of concrete, and eco-friendly materials.

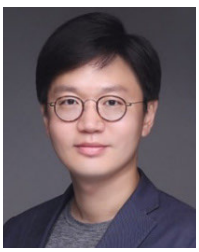

ICK-JAE YOON (Member, IEEE) received the B.S. and M.S. degrees from Yonsei University, Seoul, South Korea, in 2003 and 2005, respectively, and the Ph.D. degree from The University of Texas at Austin, Austin, TX, USA, in 2012, all in electrical engineering. From 2005 to 2008, he worked as a Research Engineer with the Samsung Advanced Institute of Technology, Samsung Electronics Company Ltd., Yongin, South Korea. From 2012 to 2014, he was with the Electromagnetic Systems Group, Department of Electrical Engineering, Technical University of Denmark (DTU), Lyngby, Denmark, as a Postdoctoral Research Fellow and an Assistant Professor. He joined the Faculty of Chungnam National University, Daejeon, South Korea, in 2014. He is currently an Associate Professor with the Department of Electrical Engineering. His current research interests include antennas, RF/microwave circuits, EMI/EMC problems from vehicles, and theoretical methods for electromagnetics. He received the H. C. Ørsted Postdoctoral Fellowship from DTU, in 2012.